PERGAMON

Atmospheric Environment 33 (1999) 2689–2698

ATMOSPHERIC ENVIRONMENT

Carbonaceous aerosol in jet engine exhaust: emission characteristics and implications for heterogeneous chemical reactions

A. Petzold[a,*], J. Ström[b], F.P. Schröder[a], B. Kärcher[a]

[a]*Deutsches Zentrum für Luft- und Raumfahrt, Institut für Physik der Atmosphäre, Oberpfaffenhafen, D-82234 Wessling, Germany*
[b]*Department of Meteorology, Stockholm University, S-10696 Stockholm, Sweden*

Received 24 September 1997; accepted 2 July 1998

Abstract

Characteristic parameters of black carbon aerosol (BC) emitted from jet engine were measured during ground tests and in-flight behind the same aircraft. Size distribution features were a primary BC mode at a modal diameter $D \approx 0.045$ μm, and a BC agglomeration mode at $D < 0.2$ μm. The total BC number concentration at the engine exit was 2.9×10^7 cm^{-3} with good agreement between model results and in-flight measured number concentrations of non-volatile particles with $D \geqslant 0.014$ μm. A comparison between total number concentration of BC particles and the non-volatile fraction of the total aerosol at the exit plane suggests that the non-volatile fraction of jet engine exhaust aerosol consists almost completely of BC. In-flight BC mass emission indices ranged from 0.11 to 0.15 g BC (kg fuel)$^{-1}$. The measured in-flight particle emission value was $1.75 \pm 0.15 \times 10^{15}$ kg^{-1} with corresponding ground test values of $1.0–8.7 \times 10^{14}$ kg^{-1}. Both size distribution properties and mass emission indices can be scaled from ground test to in-flight conditions. Implications for atmospheric BC loading, BC and cirrus interaction and the potential of BC for perturbation of atmospheric chemistry are briefly outlined.

Keywords: Black carbon; Soot; Jet exhaust aerosol; Aircraft emissions; Tropopause region; Heterogeneous chemistry

1. Introduction

Atmospheric particulate black carbon (BC), also termed soot, which is observed up to altitudes of 20 km, is an ubiquitous tracer for emissions from incomplete combustion processes. Reported BC number concentrations in the upper troposphere and lower stratosphere vary from 0.005 to 0.42 cm^{-3} with an average value of 0.1 cm^{-3} (Chuan and Woods, 1984; Pueschel et al., 1992, 1997; Sheridan et al., 1994; Blake and Kato, 1995). Corresponding BC mass concentrations are of the order of 1 ng m^{-3}.

Despite these low concentration values, BC has recently gained increasing interest due to the possible reduction of HNO_3 and NO_2 on the carbon aerosol surface (Lary et al., 1997) and to its possible role in the observed ozone depletion at middle latitudes in the northern hemisphere (Bekki, 1997). Additionally, Jensen and Toon (1997) discussed the effects of BC aerosol on the formation of cirrus clouds by changing the threshold conditions for cirrus cloud formation.

*Corresponding author. Tel.: +49 8153 28 2592; fax: +49 8153 28 1841; e-mail: andreas.petzold@dlr.de.

1352-2310/99/$ - see front matter
PII: S1352-2310(98)00314-8

Because there is no atmospheric source of BC aerosol, commercial aircraft exhaust is assumed to be the major source of BC in the upper troposphere/lower stratosphere. This assumption is supported by the strong asymmetrical distribution of BC in the northern and the southern hemisphere, which shows the highest BC concentrations in northern hemispheric middle latitudes (Pueschel et al., 1997). A comparable hemispherical distribution is obtained from model calculations by Bekki (1997). Presently, it is not possible to quantify the commercial air traffic contribution to the atmospheric BC loading of the tropopause region, because only little is known about the residence time of BC aerosol and the interaction of BC particles with other aerosols in these parts of the atmosphere, and also the emission index of BC (EI_{BC}), given in g BC (kg fuel)$^{-1}$, is not well known for the different aircraft in operation.

In a review on the effects of aircraft emissions on the atmosphere, Schumann (1994) reported EI_{BC} between 0.007 and 0.03 g kg^{-1}. From measurements behind the Concorde supersonic aircraft, Pueschel et al. (1997) estimated an EI_{BC} of 0.07 ± 0.05 g kg^{-1} and an average stratospheric BC mass loading of 0.5 ng (standard m)$^{-3}$ caused by the current subsonic aircraft fleet. Major parameters of the BC size distribution inside the Concorde plume at an average plume age of 1430 s were a number concentration of 0.21 cm^{-3}, a geometric mean diameter of 0.18 μm and a geometric standard deviation (GSD) of 1.52. The average Concorde emission index for non-volatile particles with diameter $D \geqslant 0.01$ μm (EI_{PART}, given in particles (kg fuel)$^{-1}$) was 7.2×10^{16} kg^{-1} (Fahey et al., 1995), suggesting the presence of a second BC particle mode at smaller sizes that could not be detected by the sampling method applied by Pueschel et al. (1997). The exhaust aerosol of more common subsonic commercial jet aircraft emissions was characterized by Hagen et al. (1996) with respect to total particle emission and size distribution during ground tests and in flight (≈ 8 km behind emitting aircraft). They reported log-normal size distributions with modal diameters at 0.03–0.06 μm and an average GSD of 1.6. In flight, they observed also a larger particle fraction between 0.1 and 0.2 μm. The same research group performed aerosol characterization measurements in a test cell (Howard et al., 1996). They obtained count median diameter (CMD) values of 0.03–0.04 μm and estimated emission values $EI_{PART} = 2.20 \pm 0.7 \times 10^{13}$ kg^{-1} and $EI_{BC} = 0.012 \pm 0.001$ g kg^{-1}, respectively. Schumann et al. (1996) reported estimated emission indices $EI_{BC} \approx 0.5$ g kg^{-1} and $EI_{PART} \approx 2 \times 10^{15}$ kg^{-1} for the ATTAS research aircraft of the DLR (Deutsches Zentrum für Luft- und Raumfahrt).

Summarizing the present knowledge on the BC emission from commercial aircraft, the EI_{BC} varies from < 0.01 to 0.5 g kg^{-1} and EI_{PART} is about 10^{15} kg^{-1}. The BC exhaust aerosol size distribution peaks at a modal diameter of 0.05 μm and shows a second mode at a diameter of approx. 0.2 μm. But up to now, it is not clear whether all emitted non-volatile particles are BC particles, and also their chemical nature is not known very well because most available BC emission indices are derived indirectly from size distribution measurements, assuming all particles to be spherical and of known particle density. Another important question is, to what extent ground test data can be scaled to in-flight conditions at higher altitudes.

In the following we present results from ground-based and in-flight aerosol measurements behind the ATTAS research aircraft and related measurements made behind commercial aircraft and in cirrus clouds. The studies attempt to combine airborne measurements of the exhaust aerosol size distribution and chemical analyses of aircraft-sampled contrail and cirrus crystal residuals with ground-based measurements of aerosol size distribution and chemical composition to obtain a more detailed picture of the jet engine exhaust aerosol than is available today.

2. Experimental details

The following results are based on a series of experimental flights which were conducted in 1996 and 1997 behind the ATTAS research aircraft of DLR above southern Germany. As platform for the scientific equipment the Falcon from DLR was used, which followed the ATTAS within flight distances from $\leqslant 300$ to 3000 m. The ATTAS is a medium-sized aircraft of type VFW 614, which is equipped with 2 Rolls-Royce/SNECMA M45H Mk501 turbofan engines (wing span: 21.5 m; construction year: 1971). The ATTAS exhaust and plume properties are well characterized (Schumann, 1995; Busen and Schumann, 1995; Schumann et al., 1996) which allows a more detailed analysis of the exhaust aerosol measurements.

Ground-based measurements were performed with the ATTAS being operated at different engine thrust levels. The exhaust aerosol was sampled on filter substrates which were analyzed on the content of total carbon (TC) and BC by a thermal technique (Petzold and Niessner, 1995; Petzold and Schröder, 1998); filter sampling times were < 5 min during the ground test studies. The applied analytical method uses solvent extraction and heating of the filter sample in an oxygen-free atmosphere to remove organic compounds from the filter sample. Subsequently, the BC content of the deposited aerosol is determined from the evolving CO_2 during sample combustion. Hence, the carbonaceous fraction can be split into an organic, i.e. soluble and volatilizable, and a BC fraction which is defined as insoluble, thermally stable up to 500°C in a non-oxidizing atmosphere, and strongly light-absorbing (Petzold and Niessner, 1995). This

procedure allows only a rough but yet important classification of carbonaceous exhaust aerosol.

The exhaust aerosol size distribution was measured with a standard PCASP-100X (PMS Inc.). To achieve realistic BC size channel limits for the PCASP in operation we characterized the instrument with monodisperse di(2-ethylhexyl) sebacate particles (refractive index $1.448 + 0i$) and converted the derived channel thresholds to BC size channel limits via Mie scattering values for a refractive index of $2 + 0.6i$ (see Table 1). More details on the ground test studies are given by Petzold and Schröder (1998).

In-flight aerosol characterization inside the exhaust plume of the ATTAS was performed during the SULFUR 5 campaign in 1997. The instrumentation used for the measurement of the exhaust aerosol on-board the Falcon were two modified CNC of model TSI 3760A (TSI Inc.) with experimentally determined lower cutoff diameters of 0.005 and 0.014 μm, which were connected to a dilution unit (dilution ratio 1:40) to provide full system operation also at very high CN concentrations. Additionally, the sampling line was split into a heated (200°C) and a non-heated section for alternate detection of volatile and non-volatile particles. A deiced PCASP-100X was mounted at a wing station, to size the almost dry accumulation mode aerosol in the diameter range $0.1 < D < 1.8$ μm.

Aircraft sampling of residual particles from evaporated ice crystals was performed using a Counterflow Virtual Impactor (Ogren et al., 1985) during the AEROCONTRAIL campaign in 1996. Sampling was conducted behind commercial aircraft within a flight distance of approx. 10 km. The samples were analyzed with a scanning electron microscope which was equipped with a windowless energy-dispersive X-ray detector; for details see Petzold et al. (1998).

All measurements were bound to the upper troposphere and the tropopause region with ambient air temperatures of 215–235 K. For the characterization of the dry exhaust aerosol, only those sequences of SULFUR 5 flight were analyzed, where no contrail was formed, because at contrail forming conditions, the PCASP size spectra were disturbed by break-up artifacts of contrail particles. A summary of experimental details is given in Table 2.

Table 1
PCASP particle size thresholds for an absorbing material (refractive index $2 + 0.6i$), obtained from experimentally derived channel thresholds and Mie calculations

Channel	Particle size threshold (μm)
1	0.097–0.11
2	0.11–0.13
3	0.13–0.16
4	0.16–0.18
5	0.18–0.22
6	0.22–0.29
7	0.29–1.8

3. Results and discussion

In order to compare measurements at different flight distances and ambient conditions with measurements at ground close to the nozzle exit plane of the jet engine, all concentration values were corrected to standard conditions. The plume dilution d as a function of plume age t was derived from visual observations of the plume cross section at different flight distances during previous ATTAS flights (Schumann et al., 1996). The dilution was defined as the observed plume cross section divided by the engine exit nozzle cross-sectional area of 0.125 m^2. Linear regression analysis between flight distance x (in m) and plume dilution d yielded the relation

$$d = 19 + 0.655\ \mathrm{m}^{-1}\ x \quad (1a)$$

Table 2
Analyzed measurement sequences during SULFUR 5 behind the ATTAS; all measurements were performed with fuel sulfur contents of 6 ppm (low sulfur) and 2700 ppm (high sulfur) in plumes without visible contrails

Date	FL (hft)	V ($m\ s^{-1}$)	T (K)	p (hPa)	m_f ($kg\ s^{-1}$)	x (m)	d
14 March 1996	Ground; idle run		281	950	0.05[a]	1.5	2[b]
14 March 1996	Ground; take-off		281	950	0.5[a]	1.5	20[b]
18 April 1997	260	157–164	231	357	0.151	237	197

[a] Values are taken from Schumann (1995).
[b] Values are taken from Petzold and Schröder (1998).
Abbreviations are FL, flight level; V, true air speed; T, static air temperature; p, ambient pressure; m_f, fuel flow rate per engine; x, flight distance; d, plume dilution relative to the engine exit plane.

while the dilution function (plume age t in s)

$$\delta(t) = \left[\frac{0.005}{t}\right]^{0.9} \quad (1b)$$

was derived from a numerical jet plume model constrained by CO_2 measurements (Kärcher and Fabian, 1994). As can be seen in Fig. 1 the inverse plume dilution d^{-1} according to Eq. (1a) and the dilution function $\delta(t)$ from Eq. (1b) are consistent within plume ages $t < 10$ s. For the conversion of flight distance into plume age an average flight speed of 160 m s^{-1} was used. From a comparison of relations (1a) and (1b) we estimated an average uncertainty in the dilution factor of 15% at plume ages $t \leqslant 2$ s.

BC mass emission indices EI_{BC} were obtained from measured mass concentration values C_{BC} via the relation

$$EI_{BC} = \frac{C_{BC}}{\rho_{air}} N \quad (2)$$

with C_{BC}, black carbon mass concentration at the nozzle exit plane, ρ_{air}, density of air at measurement conditions and N, air-to-fuel ratio for given combustion conditions. Equation (2) uses emitted BC mass per emitted air mass for a given amount of consumed fuel, which corresponds to a mixing ratio and is thus not affected by temperature and pressure changes from exit plane conditions to measurement conditions.

3.1. Ground test results

From the ground test studies a rough classification of the carbonaceous aerosol fraction in jet engine exhaust and on EI_{BC} was obtained as a function of engine power setting. Fig. 2 shows the increase of the BC fraction of TC with increasing engine thrust level. The BC/TC ratio varies from 10% at idle run conditions ($\leqslant 10\%$ power setting) to $> 80\%$ close to take-off thrust, which can be explained by the decreasing air/fuel ratio at increasing thrust level. Corresponding C_{BC} and EI_{BC} are given in Table 3, while Fig. 3 shows the dependence of EI_{BC} on the engine thrust level. As can be seen in Fig. 3, BC emission characteristics are affected by the fuel sulfur content only to a minor extent. These ground test values for C_{BC} and EI_{BC} will be taken as reference values in the following discussion of size distribution properties of the BC exhaust aerosol at ground and in flight.

3.2. Total number concentrations

Total aerosol number concentrations inside the ATTAS exhaust plume were measured during the SULFUR 5 flight at distances of 145–266 m with two CNC with lower cutoff diameters 0.005 and 0.014 μm. From these concentration measurements the quantities N_5 and N_{14}, which are the number concentrations of particles with $D \geqslant 0.005$ μm and $D \geqslant 0.014$ μm, respectively, were derived. In contrast, N_{MODEL} refers to the total number concentration obtained from log-normal model size distributions which were adapted to measured exhaust aerosol size distributions.

In order to characterize BC particle emissions we discriminated between total aerosol with size $D \geqslant 0.005$ μm and non-volatile particles with $D \geqslant 0.014$ μm. The latter fraction was measured with the sampling line being heated to 200°C and counted by the N_{14} counter. Sampling with a non-heated line gives the number concentration of volatile plus non-volatile particles which contains

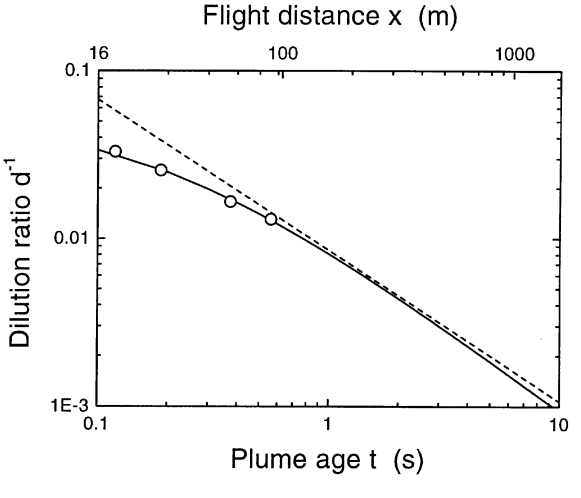

Fig. 1. Dilution ratio inside the ATTAS plume as a function of flight distance x or plume age t, respectively; the straight line corresponds to the dilution function fitted to plume cross-section observations (circles), while the broken line is obtained from a numerical jet plume model.

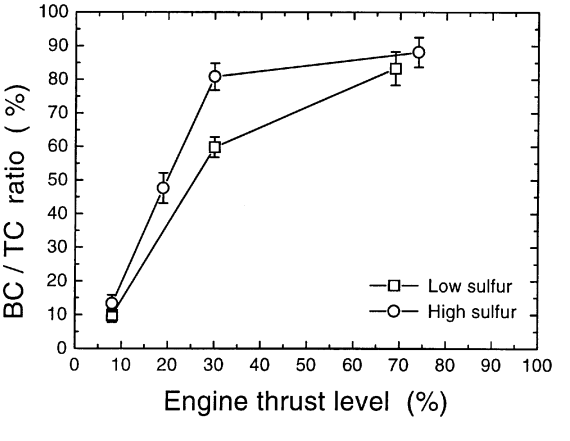

Fig. 2. Black carbon (BC) fraction of total carbon (TC) plotted as a function of engine power setting; low and high sulfur fuel values correspond to fuel sulfur contents 6 and 2700 ppm, respectively.

Table 3
Mass concentration C_{BC} and mass emission index EI_{BC} of BC in the ATTAS exhaust (ground test) at different engine thrust levels and for in-flight conditions (FL 260), specified by the fuel flow m_f and respective air fuel ratio N; values are obtained from filter sample analysis (ground test) and size distribution analysis (in-flight)

	Thrust level (%)	m_f (kg s^{-1})	N	C_{BC} (mg m^{-3})	EI_{BC} (g kg^{-1})
Ground test					
	8	0.057	70	0.26	0.015
	19	0.1	70	0.8	0.047
	30	0.146–0.151	70	2.0–2.5	0.118–0.149
	69	0.328	60	5.4	0.272
	74	0.354	60	5.6	0.333
In-flight					
FL 260	≈30	0.151	70	1.9–2.5	0.11–0.15

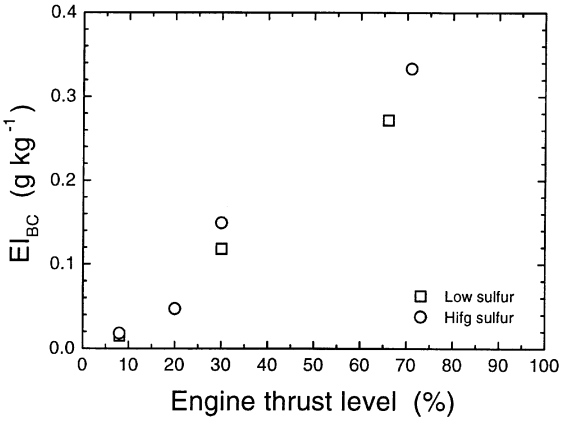

Fig. 3. Black carbon mass emission index EI_{BC} in g BC per kg fuel as a function of engine thrust level.

also a large fraction of aqueous sulfuric acid droplets (Kärcher et al., 1996). During the measurement flights only the non-volatile N_{14} fraction was observed to be almost independent from the fuel sulfur content. Because the fuel sulfur independence of BC emissions is one important result from the ground-based measurements, we interpret the non-volatile N_{14} values as BC number concentrations. Particle concentration values N_{14} corrected to engine-exit-conditions were $\approx 3 \times 10^7$ cm^{-3} for both low and high fuel sulfur content while the total N_5 values, i.e., volatile plus non-volatile particles, were 4×10^8 and 2×10^9 cm^{-3} for low and high fuel sulfur, respectively.

3.3. Size distributions

Size distributions were measured both during the ground test and in flight with the PCASP. Due to the limited size range of the PCASP (0.1 μm $< D <$ 1.8 μm), log-normal size distributions were fitted to the experimental data in order to obtain information also on the size range below the lower size limit of the PCASP. The reliability of these model distributions was checked by comparing integral properties like total mass concentration or total number concentration of the model size distributions to independently obtained experimental values like non-volatile N_{14} as measured with the CNC and C_{BC} values obtained from filter samples. This procedure does not prove the correctness of the models but gives a consistent relation between the different moments of the size distribution. Major parameters CMD, GSD, C_{BC} and N_{MODEL} are summarized in Table 4. In Fig. 4, the results of the fitting procedure in case of the flight at FL 260 on 18 April 1997 are shown. The obtained size distribution parameters indicate that 95% of the BC particles are larger than 0.011 μm in diameter.

For comparison, Hagen et al. (1996) and Howard et al. (1996) reported a modal diameter of 0.03–0.04 μm for the primary non-volatile aerosol fraction. Some spectra also show a second coagulation mode between 0.1 and 0.2 μm. Hence, these findings are in very good agreement with our size distribution results.

The comparison of size distribution parameters in Table 4 from ground test and in-flight measurements indicate that characteristic features of the BC size distribution are almost independent of altitude, i.e. from pressure and temperature. This assumption is supported by the size distributions summarized in Fig. 5, where results are plotted from the ground test and in-flight measurements during SULFUR 5 flights. It is obvious that idle run and take-off size distributions are the upper and lower bound of in-flight measured size distributions. The difference between the size distributions is caused rather by different engine thrust levels than by altitude effects on engine properties.

Table 4
Parameters of the model size distributions at different engine power settings

Parameter		Idle run ground test	Take-off ground test	In-flight (18 April 1997)	Experimental data
Primary mode					
CMD	(μm)	0.045	0.045	0.034	
GSD		1.5	1.5	1.55	
N_{MODEL}	(cm^{-3})	1.8×10^6	1.5×10^7	2.5×10^7	
Coagulated mode					
CMD	(μm)	—	0.180	0.160	
GSD		—	1.42	1.87	
N_{MODEL}	(cm^{-3})	—	4.5×10^5	1.9×10^4	
Dilution factor		2	20	197	
Total number N_{MODEL}	(cm^{-3})	1.8×10^6	1.5×10^7	2.5×10^7	2.9×10^7 (N_{14}, in-flight)
Total mass C_{BC}	($mg\ m^{-3}$)	0.24	6.4	1.9–2.5	0.26 (idle run) 2.0 (30% thrust) 5.6 (74% thrust)
Total surface S_{BC}	($\mu m^2\ cm^{-3}$)			2×10^5	

Note: Count median diameter, CMD; geometric standard deviation, GSD; total number concentration, N_{MODEL}; total mass concentration, C_{BC}; and total surface concentration, S_{BC}. Concentration values N_{MODEL}, S_{BC} and C_{BC} are given for engine exit conditions, i.e. they are corrected by the specified dilution factor, such that they can be compared directly to the respective experimental values.

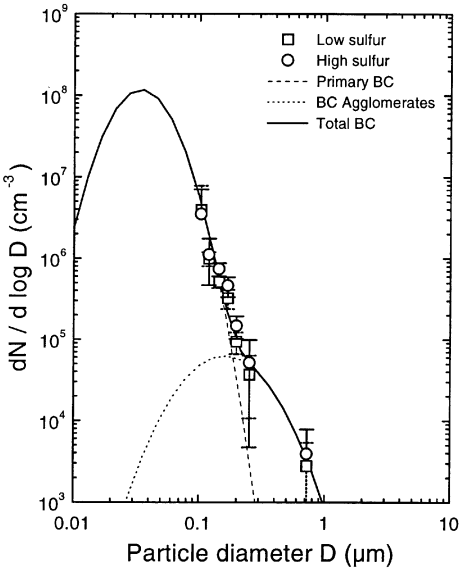

Fig. 4. Particle size distribution inside the ATTAS exhaust plume at FL 260 (flight on 18 April 1997); the parameters of the aerosol model are given in Table 4.

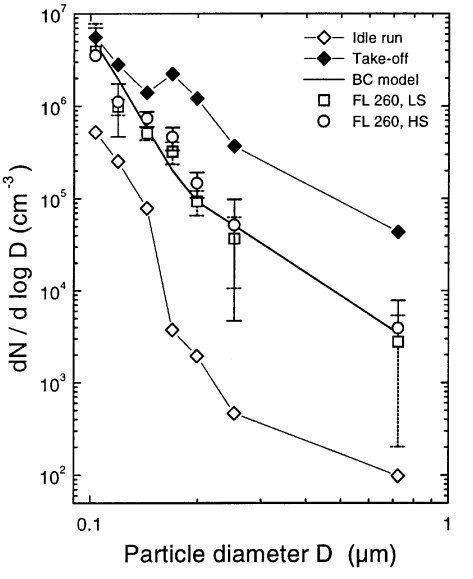

Fig. 5. Size distributions inside the ATTAS exhaust plume for different engine conditions as measured with a PCASP; HS and LS correspond to high and low fuel sulfur content, respectively.

3.4. Emission indices

In-flight BC mass emission indices were derived from the measured size distributions by applying Eq. (2) to the PCASP-measured size distributions. The weighting factor between C_{BC} derived from the PCASP-measured size spectrum (0.1 μm $< D <$ 1.8 μm) and C_{BC} of the total BC aerosol was derived empirically by relating the PCASP-measured total volume concentration times particle density $\rho_{BC} = 1.5\ g\ cm^{-3}$ to the mass concentration of the BC model aerosol for the spectra of the flight on 18 April 1997 (see also Fig. 4). This procedure yielded that the PCASP-measurable size spectrum contains 63% of the

total BC aerosol mass. Resulting C_{BC} and EI_{BC} values are given also in Table 3.

The in-flight emission indices of 0.11–0.15 g kg^{-1} compare well to a ground test value for $\approx$30% engine power setting (see Table 3), which is a reasonable value for ATTAS flight conditions with high speed at high altitude. It has to be mentioned that the in-flight emission index is obtained indirectly via the analysis of optically measured size distributions by making assumptions on particle shape and density, while the ground test emission indices are obtained directly via the chemical analysis of the emitted aerosol, which does not require any assumptions on physical and chemical properties of these particles. Therefore the very good agreement between these emission indices is noticeable.

Since the Rolls-Royce/SNECMA M45H Mk501 turbofan engine is known as emitting a huge amount of BC compared to more modern engine types, the obtained emission indices represent the upper range of mass emission indices with respect to all jet engines in service. Thus, an estimated overall emission index of 0.05 g kg^{-1} seems to be reasonable.

Another important consequence of this good agreement between ground test and in-flight emission indices as well as size distributions is the fact that characteristic parameters of jet engine BC aerosol seem to be scaleable from ground test studies to in-flight conditions. The same result was reported by Pueschel et al. (1997) for the Concorde BC aerosol.

The EI_{PART} value was calculated analogues to EI_{BC} by using Eq. (2) with N_{14} instead of C_{BC}. We obtained a value of $1.75 \pm 0.15 \times 10^{15}$ kg^{-1}. The corresponding ground test values are $1–8.7 \times 10^{14}$ kg^{-1}, while Schumann et al. (1996) estimated an in-flight value of 2×10^{15} kg^{-1} for the ATTAS. Hence, all particle emission values for the ATTAS engines agree well.

3.5. Composition of contrail and cirrus crystal residuals

Aircraft in situ sampling of ice crystal residuals was performed with a Counterflow Virtual Impactor (Ogren et al., 1985) which samples ice crystals and removes the water during sampling, such that only the dried residuals of ice crystals will be deposited on a filter matrix for subsequent analysis. Samples were taken in a contrail of a Boeing B 747, in a natural cirrus and of interstitial aerosol inside a natural cirrus. Even though this experiment did not focus on the ATTAS exhaust aerosol, we will briefly summarize the results, because some more details on the composition of BC aerosol from jet exhaust can be depicted. More details on this subject are given in Petzold et al. (1998). BC aerosol can be included into contrail crystals when BC acts as a freezing nucleus, or when BC particles are scavenged by the ice crystals (Kärcher, 1997).

In both the contrail and the cirrus residual samples BC particles were dominating the size spectrum $D < 1$ μm. The crystal residuals were accumulated in the size range $0.2\ \mu m < D < 0.5\ \mu m$ with total concentrations $N < 2\ cm^{-3}$ for cirrus samples and in the size range $0.1\ \mu m < D < 0.2\ \mu m$ with $N < 15\ cm^{-3}$ for contrail samples. Both number concentrations are common values for the respective types of ice cloud. Especially in the contrail case, the particle fraction with $D \leqslant 0.5$ μm consisted almost exclusively of carbonaceous particles with BC making up 87% of the particle mass. Coarse BC particles with $D \geqslant 1$ μm were observed only to a minor extent. All BC particles were agglomerates formed from primary spheres with a diameter well below 0.1 μm. This observation as well as the finding that the largest fraction of carbonaceous contrail crystal residuals on a number scale is in the size range $D \leqslant 0.2$ μm are in good agreement with measured BC emission size distributions.

4. Implications for atmospheric BC loading and heterogeneous reactions on exhaust BC

Implications of the observed BC aerosol properties for atmospheric BC loading are derived for the 9–13 km altitude band in the Northern Hemisphere. Approximately 60% of worldwide fuel use does occur in this altitude band (Friedl, 1997). Starting with a total amount of 1.36×10^{11} kg of fuel burned in 1992 (Friedl, 1997), an EI_{BC} value 0.05 g kg^{-1} and an average residence time of 3 months in the upper troposphere/lower stratosphere, we obtain an aircraft-related annual deposition of 4×10^9 kg BC in this part of the atmosphere, which corresponds to a BC mass loading $\leqslant 0.5$ ng m^3. The respective excess surface density is $\geqslant 0.05\ \mu m^2\ cm^{-3}$, assuming a spherical shape of the BC particles. The excess BC loading agrees well with model calculations by Bekki (1997). He reported an aircraft-related BC mass loading of 0.6 ng m^{-3} and a surface density of 0.25–0.3 μm^2 cm^{-3} in the same altitude band. The differences in the excess surface density arise from the fact that Bekki included a surface enhancement factor of 30 with respect to the fractal nature of the BC particles while our estimate is based on the assumption of spherical particles.

Given the observed variability of BC emissions, the measured size distribution and plume dilution history behind the ATTAS is comparable to other aircraft. We therefore use these parameters to evaluate the potential of BC particles to participate in heterogeneous chemistry at the flight levels. Following Kärcher (1997) the fate of the number density N of a trace gas undergoing a heterogeneous reaction (reactive uptake coefficient γ) in a spreading wake can be written as

$$\frac{dN}{dt} = -\frac{\alpha}{t}(N - N_a) - \frac{\gamma}{4} v S_{BC} N \quad (3)$$

where α is a mixing parameter, N_a is the ambient concentration (entrained into the wake at a rate αt^{-1}), $v \approx 2.5 \times 10^4$ cm s^{-1} is the molecular thermal speed, and S_{BC} is the BC surface area density. The first and second terms on the right-hand-side of Eq. (3) account for wake mixing and heterogeneous reaction, respectively. In the spreading wake, S_{BC} approaches its ambient value $S_{BC,a} \approx 0.2\ \mu m^2\ cm^{-3}$ (Blake and Kato, 1995) according to $S_{BC}(t) = S_{BC,a} + \delta(t)(S_{BC,0} - S_{BC,a})$, with the initial exit plane value $S_{BC,0} = 10^5 \mu m^2\ cm^{-3}$ from Table 4 and the dilution function $\delta(t)$ according to Eq. (1b).

Solutions of Eq. (3) imply the following assumptions: The major fraction of BC particles by number is small enough (< 0.1 μm) so that the uptake takes place in the gas kinetic regime; coagulation between BC particles is negligible. We solve Eq. (3) and investigate the chemical lifetimes τ of N prescribing a constant value of γ. Two cases are distinguished. In case 1, a trace gas is emitted by the engines (initial concentration N_0) but not entrained ($N_a = 0$). Case 2 assumes that the trace gas is present in the ambient air (concentration N_a) and is constantly mixed into the wake, but is not emitted ($N_0 = 0$). To facilitate the discussion, we plot in Fig. 6 scaled number densities corrected for wake dilution, i.e. $N\ (N_0\delta)^{-1}$ in case 1 (Fig. 6a) and $N\ [N_a\ (1-\delta)]^{-1}$ in case 2 (Fig. 6b). In the absence of chemical reactions ($\gamma = 0$), these quantities would be constant and equal to unity. Thus, any decrease of the curves in Fig. 6 is due to chemical depletion. The filled circles depict the corresponding (e-folding) lifetimes τ_1 and τ_2.

Except for $\gamma \to 1$ in case 1, τ values of emitted or entrained trace gases range between a few days up to 1 week ($\gamma \approx 0.1$), or between 1 week and a few months ($\gamma \approx 0.01$). If $\gamma > 0.1$ the reaction mainly takes place in the wake due to enhanced BC concentrations (plume lifetime is a few hours (UT) to a few days (LS)). If $\gamma < 0.1$ the chemical lifetimes are longer and mainly determined by the background BC level. For fixed γ, $\tau_1 < \tau_2$, because in case 1 no molecules are entrained into the plume and replace the ones already depleted, thereby counteracting the effect of the chemical depletion.

Among key heterogeneous reactions involving BC are a direct ozone destruction reaction ($\gamma \approx 0.001$ up to 0.03), a renoxification mechanism transforming nitric acid into nitrogen oxides ($\gamma \approx 0.02$–0.04), and reactions of SO_2 ($\gamma = 0.003$) and NO_2 ($\gamma = 0.1$) with BC, see Bekki (1997) and references therein. If we accept that even little destruction of a long-lived species like ozone or nitric acid is significant (e.g. scaled abundance drops to 0.8–0.9 in Fig. 6), we conclude that the potential of BC for perturbation of wake chemistry is quite limited and restricted to time scales between 1 day and 1 week, if $\gamma \geqslant 0.01$. Consequently, such a perturbation could especially be relevant for emissions in the lower stratosphere. This is consistent with previous estimates (Kärcher, 1997). In agreement with the more detailed calculations of Lary et al. (1997) and Bekki (1997), the impact of background BC could be more significant on a global scale.

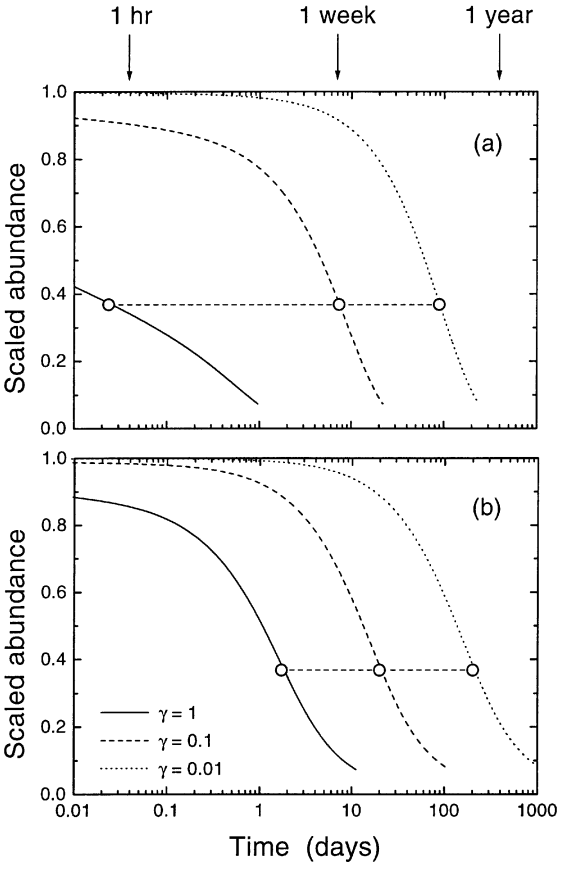

Fig. 6. Concentrations versus time of a species undergoing a heterogeneous chemical reaction with a reactive uptake coefficient γ in a diluting exhaust wake. The scaled abundance is corrected for wake mixing (no change would be seen for $\gamma = 0$). (a) and (b) show the decay due to chemical depletion of a trace gas which is only emitted by the jet engines or only entrained from the ambient air, respectively. Time values below the open circles denote the e-folding times belonging to the different γ values. For long-lived species, such as ozone, depletion of a few percent would already be significant.

Most uptake coefficients have been measured on amorphous, dry carbon surfaces in the laboratory, so the question whether these values can be directly applied to atmospheric BC is open. In this regard, the formation of a liquid surface coating due to exhaust sulfuric species is of special importance (Kärcher, 1998). It may shut off the above-mentioned reactions by occupying chemically active sites. On the other hand, other chemical reactions may then take place in the liquid coating, perhaps catalyzed by the BC particle surface. Of course, the present analysis neglects the variability of background

conditions along the exhaust trajectory and possible surface saturation effects that may affect γ. Drawing more robust conclusions about the role of exhaust BC in atmospheric chemistry will require the use of global models that consider the full set of gas phase, heterogeneous, and photolysis reactions, together with reliable BC emission inventories.

5. Summary and conclusions

The characterization of BC aerosol from jet exhaust of the ATTAS research aircraft with different techniques during ground test studies as well as in-flight yielded a rough classification of the chemical nature and a detailed picture of the size distribution of this aerosol type. Combining all results from filter sample analysis, number concentration measurements with a CNC supplied with a heated sampling line, and optical particle sizing with a deiced PCASP-100X, the fraction of non-volatile particles with $D > 0.014$ μm can be interpreted as BC exhaust particles. The size distribution features are a log-normal primary BC mode at a CMD of about 0.045 μm and a GSD ≈ 1.5, and a log-normal agglomeration particle mode at a CMD < 0.2 μm with GSD $\leqslant 1.87$. These size distribution parameters were found in ground based as well as in airborne measurements. The in-flight BC mass emission index is about 0.11–0.15 g kg^{-1} while the in-flight emission value for non-volatile particles larger than 0.014 μm in diameter is $1.75 \pm 0.15 \times 10^{15}$ kg^{-1}. For the in-flight values show good agreement with ground based data, particle emission characteristics seem to be scaleable from ground test to in-flight conditions.

The chemical composition and morphology of contrail crystal residuals agrees with the assumption that the exhaust aerosol in the size range $D \leqslant 0.5$ μm consists of BC agglomerates which are made up from smaller spheres of the above-mentioned primary BC mode in the exhaust aerosol. The second mode of agglomerated BC particles in the exhaust aerosol is also observed in the contrail crystal residuals consistent with the model predictions that small BC clusters participate in contrail formation (Kärcher et al., 1996). BC particles found as residues in cirrus crystals are indicative of BC and cirrus interaction in the upper troposphere, although our present knowledge is insufficient to ascertain the potential impact of aircraft exhaust BC on cirrus clouds.

Regarding the BC emissions of the ATTAS as typical for commercial aircraft, the potential of BC for perturbation of wake chemistry is limited and restricted to time scales between 1 day and 1 week, if reactive uptake coefficients exceed 0.01. The impact of background BC could be more significant on a global scale. Aircraft-induced perturbations are especially relevant for emissions in the lower stratosphere.

Acknowledgements

The authors are grateful to U. Schumann and R. Busen from DLR for initiating and organizing the SULFUR experiments. These projects were part of the research program "Schadstoffe in der Luftfahrt" of the German Research Ministry BMBF. Also the support of the AEROCONTRAIL crew and the flight department of DLR are gratefully acknowledged. The AEROCONTRAIL project is funded by EU.

References

Bekki, S., 1997. On the possible role of aircraft-generated soot in the middle latitude ozone depletion. Journal of Geophysical Research 102, 10 751–10 758.

Blake, D.F., Kato, K., 1995. Latitudinal distribution of black carbon soot in the upper troposphere and lower stratosphere. Journal of Geophysical Research 100, 7195–7202.

Busen, R., Schumann, U., 1995. Visible contrail formation from fuels with different sulfur contents. Geophysical Research Letters 22, 1357–1360.

Chuan, R.L., Woods, D.C., 1984. The appearance of carbon aerosol particles in the lower stratosphere. Geophysical Research Letters 11, 553–556.

Fahey, D.W. et al., 1995. Emission measurements of the Concorde supersonic aircraft in the lower stratosphere. Science 270, 70–74.

Friedl, R.R. (Ed.), 1997. Atmospheric Effects of Subsonic Aircraft: Interim Assessment Report of the Advanced Subsonic Technology Program. NASA Reference Publication 1400, NASA Center for Aerospace Information, Linthicum Heights.

Hagen, D.E., Whitefield, P.D., Schlager, H., 1996. Particle emissions in the exhaust plume from commercial jet aircraft under cruise conditions, Journal of Geophysical Research 101, 19 551–19 557.

Howard, R.P., Hiers, R.S., Whitefield, P.D., Hagen, D.E., Wormhoudt, J.C., Miake-Lye, R.C., Strange, R., 1996. Experimental characterization of gas turbine emissions at simulated flight altitude conditions. AEDC-TR-96-3, Arnold Engineering Development Center, Technical Report, NTIS, September 1996.

Jensen, E.J., Toon, O.B., 1997. The potential impact of soot particles from aircraft exhaust on cirrus clouds. Geophysical Research Letters 24, 249–252.

Kärcher B., 1997. Heterogeneous chemistry in aircraft wakes: constraints for uptake coefficients. Journal of Geophysical Research 102, 19 119–19 135.

Kärcher, B., 1998. On the potential importance of sulfur-induced activation of soot particles in nascent jet aircraft exhaust plumes, Atmospheric Research 46, 293–305.

Kärcher. B., Fabian, P., 1994. Dynamics of aircraft exhaust plumes in the jet-regime. Annals of Geophysics 12, 911–919.

Kärcher, B., Peter, Th., Biermann, U.M., Schumann, U., 1996. The initial composition of jet condensation trails. Journal of Atmospheric Science 53, 3066–3083.

Lary, D.J., Lee, A.M., Toumi, R., Newchurch, M.J., Pirre, M., Renard, J.B., 1997. Carbon aerosols and atmospheric photochemistry. Journal of Geophysical Research 102, 3671–3682.

Ogren, J.A., Heintzenberg, J., Charlson, R.J., 1985. In situ sampling of clouds with a droplet to aerosol converter. Geophysical Research Letters 12, 121–124.

Petzold, A., Niessner R., 1995. Method comparison study on soot-selective techniques. Mikrochim. Acta 117, 215–237.

Petzold, A., Schröder, F.P., 1998. Jet engine exhaust aerosol characterization. Aerosol Science Technology 28, 62–76.

Petzold, A., Busen, R., Schröder, F.P., Baumann, R., Kuhn, M., Ström, J., Hagen, D. E., Whitefield, P.D., Baumgardner, D., Arnold, F., Borrmann, S., Schumann, U., 1997. Near field measurements on contrail properties from fuels with different sulfur content. Journal of Geophysical Research 102, 29 867–29 880.

Petzold, A., Ström, J., Ohlsson, S., Schröder, F.P., 1998. Elemental composition and morphology of ice crystal residual particles in cirrus clouds and contrails. Atmospheric Research 49, 21–34.

Pueschel, R.F., Blake, D.F., Snetsinger, K.G., Hansen, A.D.A., Verma, S., Kato, K., 1992. Black carbon (soot) aerosol in the lower stratosphere and upper troposphere. Geophysical Research Letters 19, 1659–1662.

Pueschel, R.F., Boering, K.A., Verma, S., Howard, S.D., Ferry, G.V., Goodman, J., Allen, D.A., Hamill, P., 1997. Soot aerosol in the lower stratosphere: pole-to-pole variability and contribution by aircraft. Journal of Geophysical Research 102, 13 113–13 118.

Schumann, U., 1994. On the effect of emissions from aircraft engines on the state of the atmosphere. Annals of Geophysics 12, 365–384.

Schumann, U., 1995. Jet engine exit conditions derived from budget analysis for the ATTAS-M45H and other engines. Internal Report 553-3/95, DLR, Oberpfaffenhofen.

Schumann U., Ström, J., Busen, R., Baumann, R., Gierens, K., Krautstrunk, M., Schröder, F.P., Stingl, J., 1996. In situ observations of particles in jet aircraft exhausts and contrails for different sulfur-containing fuels. Journal of Geophysical Research 101, 6853–6869.